Polymer Chemistry

PAPER

View Article Online
View Journal | View Issue

Cite this: *Polym. Chem.*, 2019, **10**, 5094

Block copolymers containing stable radical and fluorinated blocks with long-range ordered morphologies prepared by anionic polymerization†

Alicia Cintora,[a] Hiroki Takano,[b] Mohit Khurana,[a] Alvin Chandra,[b] Teruaki Hayakawa[b] and Christopher K. Ober*[a]

We report a facile synthetic approach to create stable radical block copolymers containing a secondary fluorinated block *via* anionic polymerization using a bulky, sterically hindered countercation composed of a sodium ion and di-benzo-18-crown-6 complex. The synthetic conditions described in this report allowed for controlled molecular weights and dispersity (<1.3) of both homopolymers: poly(2,2,6,6-tetramethyl-1-piperidinyloxy-methacrylate) (PTMA) and poly(2,2,2-trifluoroethyl methacrylate) (PTFEMA) as well as their block copolymers (PTMA-*b*-PTFEMA). The stable radical concentration of the polymers was determined by electron spin resonance (ESR) and showed radical content above 70%. An analysis of the microphase morphologies in PTMA-*b*-PTFEMA thin films *via* atomic force microscopy (AFM) and grazing incidence small angle X-ray scattering (GISAXS) showed clear evidence of long-range ordering of lamellar and cylindrical morphologies with 32 and 36 nm spacing, respectively. The long-range ordering of the morphologies was developed with the aid of two separate neutral layers: PTMA-*ran*-PTFEMA-*ran*-poly(hydroxyl ethyl methacrylate) (PHEMA) and poly(isobutyl methacrylate) (PiBMA)-*ran*-PTFEMA-*ran*-PHEMA, which helped us corroborate, along with the Zisman method, the surface energy estimation of PTMA to be 30.1 mJ m^{-2}.

Received 16th March 2019,
Accepted 15th August 2019

DOI: 10.1039/c9py00416e

rsc.li/polymers

Introduction

Over the past twenty years, stable radical polymers, such as poly(TEMPO-methacrylate) (PTMA), have been largely associated with active cathode materials in organic rechargeable batteries.[1–5] PTMA has shown to be an advantageous polymer that offers improvement in power density compared to lithium-ion batteries due to its fast redox kinetics. However, its redox behavior has been greatly aided by the use of electrolyte solutions for efficient electron transport. Emerging work has now found applications of stable radical polymers in solid-state devices ranging from layered memory devices, where a PTMA film (as a p-type layer) and a galvinoxyl polymer film (as an n-type layer) led to bistable electroconductivity,[6] to organic photovoltaic (OPV) devices where PTMA was incorporated as an anode layer for hole transport. The OPV device was found to improve the open circuit voltage when poly(3-hexylthiophene) and [6,6]-phenyl-C_{61}-butyric acid methyl ester were used as the electron donating layers.[7] The electrical conductivity in solid state thin films has also been explored and PTMA has been found to be an electronic insulator regardless of synthetic preparation.[8] However, when TEMPO is attached to a mobile, low T_g backbone, charge transport between pendant group to pendant group is observed at room temperature.[9]

New solid-state applications are still emerging, and in order for PTMA to be a viable material in organic electronic systems, patterning and controlling the long-range order of PTMA at the nanoscale should be fully explored. Recent reports have focused on the nanopatterning of PTMA *via* block copolymer systems, but long-range order has neither been discussed nor reported. In 2015, Boudouris *et al.* studied the phase morphologies of PDMS-*b*-PTMA synthesized by a PDMS macroinitiator *via* atom transfer radical polymerization (ATRP)[10] and Gohy *et al.* utilized the self-assembly of PS-*b*-PTMA synthesized by ATRP to create thin film cathode electrodes.[11] The morphologies of PS-*b*-PTMA and PtBMA-*b*-PTMA block copolymers

[a]*Department of Materials Science and Engineering, Cornell University, Ithaca, NY, 14853, USA. E-mail: cko3@cornell.edu*
[b]*Department of Materials Science and Engineering, School of Materials and Chemical Technology, Tokyo Institute of Technology, 2-12-1-S8-36 Ookayama, Meguro-ku, Tokyo, Japan*

†Electronic supplementary information (ESI) available: Additional NMR, SEC, thermal analysis and surface energy characterization. See DOI: 10.1039/c9py00416e

were also reported by Ober *et al.*[12] and were one of the first systems to be polymerized *via* anionic polymerization.

It is our interest to study and further control the orientation and morphology of PTMA in block copolymer systems. In order to broaden the range of materials possible, new chemistry needs to be explored. To date, most PTMA containing block copolymers have been synthesized *via* reversible-deactivation radical polymerizations (RDRP) such as reversible addition–fragmentation chain transfer (RAFT)[2] and ATRP.[13] Anionic polymerization is a preferred route as it can directly polymerize TMA and as a result, yields lower dispersity polymers with higher radical content compared to the RDRP methods previously employed. Using RDRP as a route to synthesize PTMA and its block copolymers often results in non-uniform molar mass distributions and lower radical yields. Many phase-separated structures of various di- and tri-block copolymers with broad molecular weights have been observed in the past,[14–20] and therefore, in these cases, narrow dispersities are not mandatory. However, previously employed RDRP methods to synthesize PTMA require the polymerization of an amine precursor monomer with subsequent oxidation to obtain the final nitroxide-containing PTMA. These conversion reactions do not reach full yields, and often result in additional moieties including hydroxylamino species and oxoammonium cations. Our work aims to create low dispersity PTMA *via* anionic polymerization, minimizing side reactions to the nitroxide moiety and therefore achieving high stable radical content. There are extensive examples in the literature of synthetic techniques to directly polymerize nitroxide-containing monomers, from ring-opening metathesis,[21–23] transition-metal catalysis[24,25] and cationic polymerization.[26,27] However, direct polymerization of the commonly used TEMPO-methacrylate (TMA) monomer has only been achieved *via* anionic polymerization with only the latter citation achieving low dispersities.[28–31]

The secondary block provides a handle in tuning the degree of phase segregation, in particular, the Flory–Huggins χ parameter.[32] A fluorinated polymer such as poly(2,2,2-trifluoroethyl methacrylate) (PTFEMA) is of interest because it introduces unique properties to the polymer system. Poly(fluoroalkyl methacrylate)s are known for their high thermal stability and their unique optical properties.[33–35] More importantly, however, they also have the ability to increase the χ parameter of block copolymers, allowing facile phase segregation.[32,36,37] PTFEMA is also known to be easily degradable under deep-UV or e-beam radiation,[38] furthering the applicability of the block copolymers reported in this work in nanofabrication. Various fluorinated block copolymers containing PTMA and synthesized *via* ATRP have been reported.[39] However, only modest ordering and phase separation was observed in these materials.

Although poly(fluoroalkyl methacrylate)s introduce unique properties to a system, anionic polymerization of these monomers has proven to be a challenge, as methods reported have only observed low yields or low controlled molecular weights.[40–43] Therefore, in order to be able to produce large molecular weight PTMA nanopatterns with high radical yields, we must explore new synthetic routes. In this work, we report a novel approach using anionic polymerization to synthesize both PTMA and PTFEMA homopolymers that can also create PTMA-*b*-PTFEMA block copolymers in a controlled manner *via* sequential monomer addition. We also improve the long-range ordering and self-assembly of these morphologies including lamellar and cylindrical nanostructures using neutral underlayers between the polymer/Si substrate interface. We show *via* atomic force microscopy (AFM) that we are able to create long-range ordered structures throughout the film. These results are further corroborated by GISAXS analysis of PTMA-*b*-PTFEMA thin films.

Experimental

Materials

All reagents were purchased from Sigma Aldrich. Anionic polymerizations were performed under argon atmosphere. Tetrahydrofuran (THF) was dried over calcium hydride (CaH_2), distilled into a flask containing sodium and benzophenone, and distilled once more right before use. 1,1-Diphenylethylene (DPE) was distilled from CaH_2 and kept under nitrogen in a glovebox at room temperature. 2,2,2,-Trifluoroethyl methacrylate (TFEMA) was purified twice: first it was stirred over CaH_2 and distilled. Then, it was stirred over trioctylaluminum solution, distilled once more to remove residual alcohols and stored at −6 °C under nitrogen atmosphere. Dibenzo-18-crown-6 (DB18C6) was recrystallized from acetonitrile, dried, and kept under dry air. TEMPO-methacrylate (TMA) was synthesized according to the literature,[31] dried under high vacuum for 24 hours, transferred into a glovebox to be dissolved in dry THF and kept at −6 °C under nitrogen atmosphere.

Instrumentation

All ^{1}H NMR (THF-d_8, 500 MHz, ppm) spectra were collected on a Bruker INOVA 500 NMR instrument. Size exclusion chromatography (SEC) was measured using a Tosoh EcoSEC HLC 8320GPC system with two SuperHM-M columns in series, as a flow rate of 0.350 mL min^{-1} with THF as eluent against polystyrene standards. Matrix-assisted laser desorption ionization time-of-flight mass spectrometry (MALDI-TOF-MS) was performed on a Shimadzu AXIMA Performance equipped with a nitrogen laser with a wavelength of 337 nm and an accelerating voltage of 20 kV. The film thickness of spin-coated films was measured with a Filmetrics F20 refractometer. Atomic Force Microscopy (AFM) images were obtained using an Asylum-MFP3D-Bio-AFM-SPM in tapping mode. The flattened images and Fourier Transforms were obtained using Gwyddion software. Solution-state Electron Paramagnetic Resonance (EPR) measurements were performed in a Bruker X-band EPR spectrometer at room temperature. Solutions of PTMA-*b*-PTFEMA polymers were made in THF at a 1 mM concentration of the repeat TEMPO-methacrylate unit from a stock solution

of 2.5 mg mol^{-1}. The percentage of PTMA in the stock solution was determined from NMR ratio values. Grazing Incidence Small Angle X-Ray Scattering (GISAXS) experiments were performed at the Cornell High Energy Synchrotron Source (CHESS) D1 station. A Pilatus200k detector was used to capture images, at an X-ray wavelength of 0.117 nm. All images were taken at an incident angle (α_i) of 0.15°, slightly higher than the critical angle (α_{cp}) of the polymer film. The collected GISAXS intensity maps were processed using indexGIXS and processGIXS.[44] This processing method allowed us to convert the intensity map images into reciprocal space, and index diffraction peaks that correspond to real-space dimensions.

General procedure for the synthesis of PTMA-*b*-PTFEMA block copolymers and their homopolymers

An oven dried Schlenk flask was taken directly from the oven, and 0.126 g (0.349 mmol) of DB18C6 were added. While still hot, the flask and PTFE stopcock were taken into the glovebox where 60 mL of THF were added. The solution was allowed to stir until the DB18C6 was fully dissolved. The flask was then taken out of the glovebox where it was purged for 30 minutes with argon gas and cooled to −78 °C in a dry ice/acetone bath. To remove any impurities originating from the glass, a few drops of *sec*-BuLi were added while stirring until the THF turned light yellow. The THF was then used to rinse the insides of the glassware and react with potentially present impurities. The flask was then removed from the acetone/dry ice bath and allowed to come to room temperature. The flask was then cooled to −78 °C again and 25 μL (35 μmol) of *sec*-BuLi and 25 μL (142 μmol) of DPE were added dropwise until the THF solution turned a bright orange. The solution was left to stir for 30 minutes, and 87 μL (175 μmol) of a 2 M sodium *tert*-butoxide (*tert*-BuONa) solution in THF were added. The solution was allowed to stir for an additional hour before slowly adding the predetermined volume of either TMA or TFEMA monomers. The TMA monomer was kept as a solution in dry THF at a concentration of 0.2 g mL^{-1}. For the synthesis of PTMA-*b*-PTFEMA block polymers (Scheme 1), the TMA solution was added first and allowed to proceed for 12 hours to ensure all monomer was consumed for all block copolymers reported. A 1 mL aliquot of the PTMA homopolymer in solution was taken *via* purged syringe and quenched in methanol.

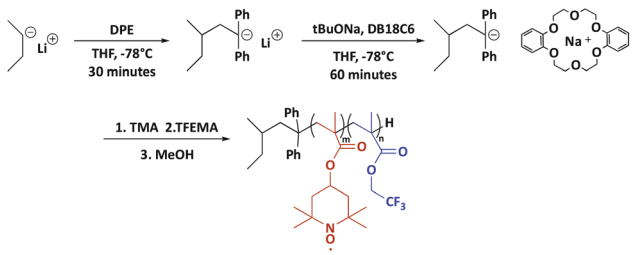

Scheme 1 Synthesis of PTMA-*b*-PTFEMA block copolymers by anionic polymerization using a Na^+/DB18C6 countercation and sequential monomer addition.

Then, the TFEMA monomer was added slowly and allowed to polymerize. The polymerization of the block copolymers and homopolymers was quenched using 1 mL of degassed methanol. To remove excess salts from the polymer, the THF was removed from the polymer solution *via* rotary evaporator. The remaining product of polymer and salts was dissolved in chloroform and washed with water 3 times before precipitating in excess cold hexanes. The block copolymer was collected by vacuum filtration as a light pink/orange powder and dried under vacuum overnight at 40 °C. PTMA-*b*-PTFEMA characteristics were determined by NMR and SEC and are listed in Table 2. All molecular weights (M_n) were determined by comparing the integrated areas of the DPE initiator peak ($\delta \sim 7.4$) *versus* the CH of the PTMA side groups ($\delta \sim 4.9$) and/or CH_2 of the PTFEMA side groups ($\delta \sim 4.5$).

Neutral layer random copolymer brushes

Random terpolymers (RTP) consisting of TFEMA, 2-hydroxyethyl methacrylate, and a third monomer (either TMA or isobutyl methacrylate (IBMA)) were synthesized *via* classical radical polymerization (CRP) according to previously reported literature procedures.[45] Random terpolymer characteristics can be found in the ESI Table S2.†

Development of nanostructure morphologies from PTMA-*b*-PTFEMA thin films

Silicon wafers were used directly from the manufacturer (WRS Materials) container. A filtered solution of α,α,α-trifluorotoluene (TFT) was spun at 1500 rpm onto a silicon substrate for rinsing. A 1 wt% solution of a random terpolymer solution in TFT was spin-coated onto the 4-inch wafers at 500 rpm for 60 seconds. The solutions gave 30–40 nm thick films. The wafer was then annealed at 150 °C in vacuum for 4 hours to allow the hydroxyl groups to covalently bond with the Si surface. The wafer was then cut into 1 cm pieces, and the unbound random copolymer chains were then removed by rinsing the wafer in TFT several times before spin-coating a 2 wt% block copolymer solution in TFT at 3000 rpm for 30 seconds. The block copolymer films spun on 1 × 1 cm sized Si wafers were then placed in a glass chamber containing 10 mL of chloroform. The glass chamber was then closed, and samples were left to anneal for 6 hours. For further details on the solvent annealing procedure, please refer to Fig. S8 in the ESI.†

Results and discussion

Synthesis of PTMA and PTFEMA homopolymers

We explored the homopolymerization of both TMA and TFEMA monomers prior to their use in block copolymers by sequential monomer addition. Typical synthetic conditions to control the anionic polymerization of many methacrylate monomers include a *sec*-BuLi/DPE initiator in the presence of excess LiCl to increase lithium association with the anion, and therefore control unwanted side reactions, such as backbit-

ing.[46] Intramolecular backbiting is a commonly known terminating side reaction of various methacrylates that has been mitigated by incorporating excess LiCl.[46–49] The side reactions are due to a nucleophilic attack of the ester group, which result in a cyclic ketone end group on the polymer chain and an alkoxide leaving group upon termination. An example of this side reaction occurring during the polymerization of TFEMA is shown in Scheme 2.

Similar conditions have been reported to suppress side reactions with the nitroxide moiety and successfully synthesize PTMA with low dispersities and high radical yields.[31] However, when these conditions were first employed to polymerize TMA and sequentially grow TFEMA, broad SEC traces with significant tailing were observed. These preliminary results allowed us to infer that while these conditions were suitable for synthesizing PTMA, competing side reactions or partial terminations were preventing the well-controlled polymerizations of TFEMA. In fact, controlling unwanted side reactions during the polymerization of TFEMA *via* anionic polymerization has been a difficult task to achieve, with previous reports in the literature suggesting that termination or chain transfer reactions were responsible for low molecular weight polymers;[40–42] however, these side reactions were never experimentally confirmed.

To determine the nature of the side reactions occurring during the polymerization of TFEMA, matrix-assisted laser desorption/ionization time-of-flight mass spectrometry (MALDI-TOF-MS) was used to characterize PTFEMA synthesized using a *sec*BuLi/DPE initiator with excess LiCl. The MALDI-TOF-MS spectrum (Fig. 1) revealed two sets of signals at approximately 168 Da intervals, suggesting the presence of two distinct species in the resulting polymer. The first set of peaks (green) appear at intervals of 168*n* + 261.39 Da, where *n* is n^{th} monomer and can be attributed to the *sec*-BuLi/DPE initiator fragment (237.39 Da), the n^{th} TFEMA monomer unit (168*n* Da), the terminal proton (1.01 Da), and a sodium cation (Na^+, 22.99 Da) (Scheme 3). The positions of these peaks suggest that the desired PTFEMA product was obtained. However, the second set of peaks (red) appear to be shifted, and appear at 168*n* + 666.68 Da. Moreover, the MALDI-TOF-MS signals upon backbiting onto the carbonyl functionality (406.3 Da) are expected to appear at 168*n* + 666.68 Da (Scheme 3). Therefore, the MALDI-TOF-MS analysis suggests that competing side reactions that involve backbiting onto carbonyl groups of PTFEMA prevented the well-controlled polymerization of TFEMA and the development of two polymers with chemically distinct end groups.

By using a bulky, sterically hindered countercation composed of a Na^+/DB18C6 complex, at a ratio of 5 : 10 with respect to the initiator, side reactions during the polymerization of TFEMA were suppressed successfully. Table 1 shows a set of PTFEMA homopolymers synthesized with molecular weights ranging from 2400–126 800 g mol^{-1} and dispersities

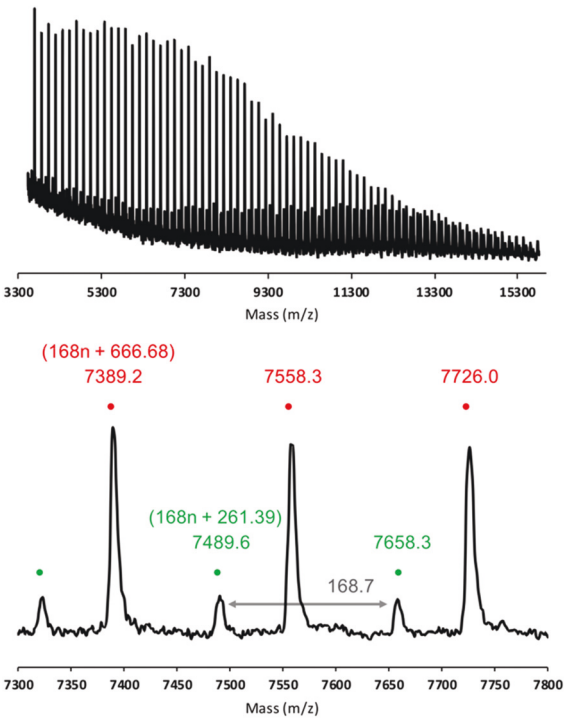

Fig. 1 MALDI-TOF-MS spectrum of PTFEMA synthesized with a Li^+ countercation with excess LiCl.

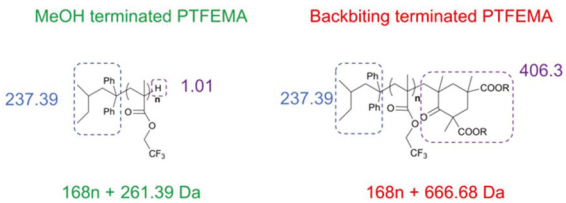

Scheme 3 Species and respective molar masses of PTFEMA chains properly terminated by degassed MeOH and those terminated due to backbiting.

Table 1 Characteristics of various PTFEMA homopolymers

Sample	$M_{n,theo.}$ [a] (g mol^{-1})	M_n [b] (g mol^{-1})	$Đ$ [c]	Time (min)	Yield [d] (%)
1	3000	2400	1.10	5	86.9%
2	20 000	19 200	1.15	5	91.4%
3	45 000	45 300	1.06	5	96.2%
4	100 000	126 800	1.14	10	96.9%

[a] Theoretical target molecular weights calculated from amount of initiator and monomer ratios added. [b] Determined by ^1H NMR (500 MHz, THD d-8). [c] Determined by SEC (THF, PS standards). [d] Yields determined post-purification.

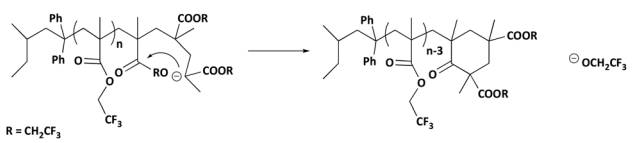

Scheme 2 Plausible termination *via* backbiting of PTFEMA.

<1.15 using these conditions, in which all reactions were complete in less than 10 minutes after quenching with degassed methanol. The low dispersities show that the side reactions initially observed were suppressed using the Na^+/DB18C6 complex as a countercation. Likewise, MALDI-TOF-MS analysis of PTFEMA synthesized with the Na^+/DB18C6 complex showed only one set of peaks at intervals of ~168 Da (Fig. S1, ESI†).

These conditions were also successful in synthesizing PTMA homopolymers, however, with much slower kinetics and slightly higher dispersities. To compare both polymerizations, aliquots of a PTMA homopolymerization, with a target molecular weight of 8000 g mol^{-1}, were taken every 15 minutes to compare the increase in molecular weight. While PTFEMA homopolymers of molecular weights up to 126 800 g mol^{-1} can be grown in 10 minutes, it requires twice the time (20 minutes) to achieve a molecular weight of only ~4800 g mol^{-1} for PTMA homopolymers as shown in Table 2. In order to be able to synthesize larger molecular weight PTMA, such as those achieved in the reported PTMA-*b*-PTFEMA samples, several hours are required for the polymerization. To ensure total consumption of TMA monomer, reactions were allowed to proceed for 12 hours. Using these conditions, the theoretical compositions were achieved. The dispersities of various PTMA homopolymers remain at an average of 1.22 even at larger molecular weights, most likely due to partial side reactions between the anion and nitroxide side group, as will be discussed in the following section.

Due to the mismatch in size between DB18C6 and the lithium countercation, from the presence of the *sec*-BuLi initiator, we do not expect any significant complexation between Li^+ and the crown ether.[50,51] Instead, *tert*-BuONa is added at 5-fold excess with respect to the initiator to form the complex with the 10-fold addition of DB18C6. Various ratios were explored to find the optimal conditions for polymerizing TFEMA (ESI, Table S1†), and a ratio of 5 : 10 Na^+/DB18C6 with respect to the initiator was found to work best.

Although the THF and crown ether both compete for solvation of Na^+ countercation in solution,[51] the favorable stability constants of the Na^+/DB18C6 complexes and excess crown ether facilitate the formation of the Na^+/DB18C6 complex.[52] When these complexes are formed, and are in excess compared to the Li^+ counterion, they solvate the propagating anion to create a bulky and steric barrier between the ion pair. The Na^+/DB18C6 complex is strong enough to polymerize both methacrylate monomers, while controlling unfavorable side reactions.[51] Using this system, both PTMA and PTFEMA homopolymers were synthesized with controlled molecular weights and dispersities.

Table 2 Molecular weight as a function of time for a PTMA homopolymerization

Sample[a]	M_n [b] (g mol^{-1})	$Đ$[c]	Time (min)
1	3100	1.25	5
2	4800	1.22	20
3	6100	1.24	35
4	6800	1.24	50

[a] Target molecular weight of the PTMA homopolymerization was 8000 g mol^{-1}. [b] Determined by ^{1}H NMR (500 MHz, THD d-8). [c] Determined by SEC (THF, PS standards).

Synthesis of block copolymers

A series of PTMA-*b*-PTFEMA block copolymers were synthesized with a broad range of molecular weights and block-to-block ratios. Using Na^+/DB18C6 complex as a bulky and sterically hindered countercation, we can successfully synthesize PTMA-*b*-PTFEMA block copolymers *via* sequential monomer addition (Fig. 2). The conditions presented in this report are the first, to our knowledge, that allow the controlled anionic polymerization of PTMA-*b*-PTFEMA by sequential monomer addition. Molecular weight and dispersity data of PTMA-*b*-PTFEMA can be seen on Table 3. Unimodal SEC traces can be found in the ESI (Fig. S4†).

Since we directly polymerize the nitroxide containing monomer, TMA, it is imperative that the stable radical yield is measured post polymerization to assess the extent of side reactions during synthesis. Stable radical content was measured using quantitative solution state electron paramagnetic resonance (EPR). Table 3 shows the stable radical percentages and show that all polymers have between 66%–80% of stable radical sites filled, indicating that side reactions between the anion and the stable radical occurred but were limited. The side reactions were likely the cause of the increase in dispersity in the PTMA homopolymers and the block copolymers containing PTMA. Similar results have been reported by Nishide *et al.*[31] where the use of an MMA-capped initiator suppressed side reactions with the stable radical, while improving the dispersity and radical concentration of PTMA homopolymers. It is important to note that attempts to improve the characteristics of the PTMA-*b*-PTFEMA block copolymers synthesized *via* the Na^+/DB18C6 system using a methacrylate capped initiator did not lead to improved dispersities or radical concentrations.

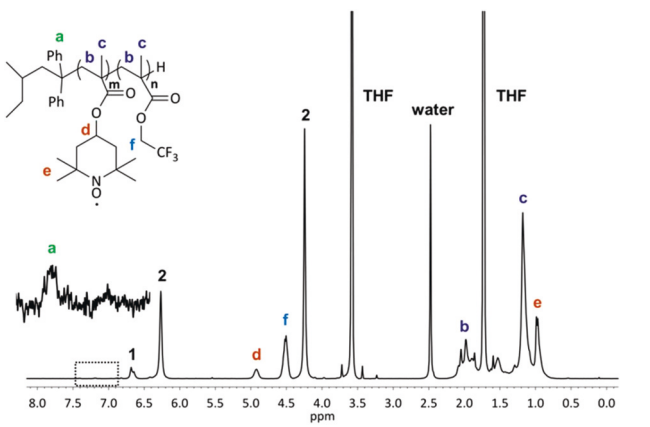

Fig. 2 ^{1}H NMR spectrum of $PTMA_{381}$-*b*-$PTFEMA_{253}$ measured in THF d-8 after reduction with pentafluorophenylhydrazine (PFPhHz). Signals attributable to the N–OH group (converted from NO$^•$) are assigned as 1. The PFPhHz signals are marked as 2.

Table 3 Molecular weight, dispersity, and radical concentration of PTMA-*b*-PTFEMA block copolymers

			NMR[b]		SEC[c]		
Sample	[I] : [TMA] : [TFEMA]	f^{th}_{TFEMA} [a]	M_n (g mol^{-1})	f^{exp}_{TFEMA}	$Đ$	Radical%[d]	Yield[e]
$PTMA_{117}$-*b*-$PTFEMA_{205}$	1 : 125 : 297	0.70	62 500	0.64	1.20	66.5%	91.4%
$PTMA_{29}$-*b*-$PTFEMA_{87}$	1 : 31 : 95	0.75	21 700	0.75	1.22	73.9%	86.5%
$PTMA_{35}$-*b*-$PTFEMA_{173}$	1 : 41 : 162	0.80	37 600	0.83	1.25	73.2%	83.3%
$PTMA_{187}$-*b*-$PTFEMA_{230}$	1 : 125 : 268	0.68	83 600	0.55	1.27	73.7%	82.1%
$PTMA_{381}$-*b*-$PTFEMA_{253}$	1 : 312 : 300	0.49	134 100	0.40	1.29	80.0%	90.6%

[a] Calculated molar fraction of PTFEMA component from monomer ratios added. [b] Determined by ^{1}H NMR (500 MHz, THF d-8). [c] Determined by SEC (THF, PS standards). [d] Determined by ESR (1 mmol solutions of PTMA component in THF). [e] Yields determined post-purification.

Phase separation in thin film studies by AFM

In this work, we utilized random terpolymers as neutral underlayers between the polymer/Si interface, synthesized *via* classical radical polymerization, to aid the long-range ordering of the PTMA-*b*-PTFEMA thin films. The first neutral underlayer, PTMA-*ran*-PTFEMA-*ran*-PHEMA (RTP-1) was synthesized using a two-step process where a precursor monomer, 2,2,6,6-tetramethyl-4-piperidinyl methacrylate (TMPM), was used and subsequently oxidized with H_2O_2/Na_2WO_4 to obtain RTP-1. A second neutral layer, PiBMA-*ran*-PTFEMA-*ran*-PHEMA, (RTP-2) was created by replacing the TMA monomer with a methacrylate monomer of similar surface energy. The surface energy of PTMA was estimated to be 30.12 mJ m^{-2} *via* a Zisman plot (ESI, Fig. S11†), therefore, IBMA (surface energy: 30.19 mJ m^{-2} (ref. 53)) was used as a substitute in the neutral layer. Monomer ratios, structures, and NMR spectra of RTP-1 and RTP-2 are reported in the ESI (Fig. S9 and S10,† respectively). Due to the low surface energy of PTFEMA, this block prefers to phase segregate to the air–polymer interface, while PTMA, due to its higher surface energy, preferentially wets the silicon substrate. This limits the long-range ordering of PTMA-*b*-PTFEMA thin films spun on bare Si wafers, and is a common phenomenon observed in various block copolymers composed of blocks with varying surface energies.[54–56]

By analyzing the annealed block copolymer thin films, the phase morphologies at the surface of the film are able to be observed. As shown in Fig. 3, disordered lamellar morphologies are obtained in $PTMA_{187}$-*b*-$PTFEMA_{230}$ (left) when no neutral underlayer is used and is annealed in $CHCl_3$ vapor for 6 hours. Likewise, the AFM images of $PTMA_{381}$-*b*-$PTFEMA_{253}$ (Fig. 3, right) show that disordered cylindrical morphologies are obtained with no neutral underlayers used. The lack of long-range order is corroborated by the Fourier transform (FFT) images for each film in which no underlayer was used. To obtain long range order in these nanostructures, neutral layers between the Si/block copolymer interface, are needed to enable preferential wetting of both blocks during phase separation.

$PTMA_{187}$-*b*-$PTFEMA_{230}$ showed an increase in the interconnectedness of the lamellar structures when an underlayer was used and is confirmed by the pattern alignment of the FFT image. Likewise, the hexagonal packing of the cylindrical structures of $PTMA_{381}$-*b*-$PTFEMA_{253}$ was also improved.

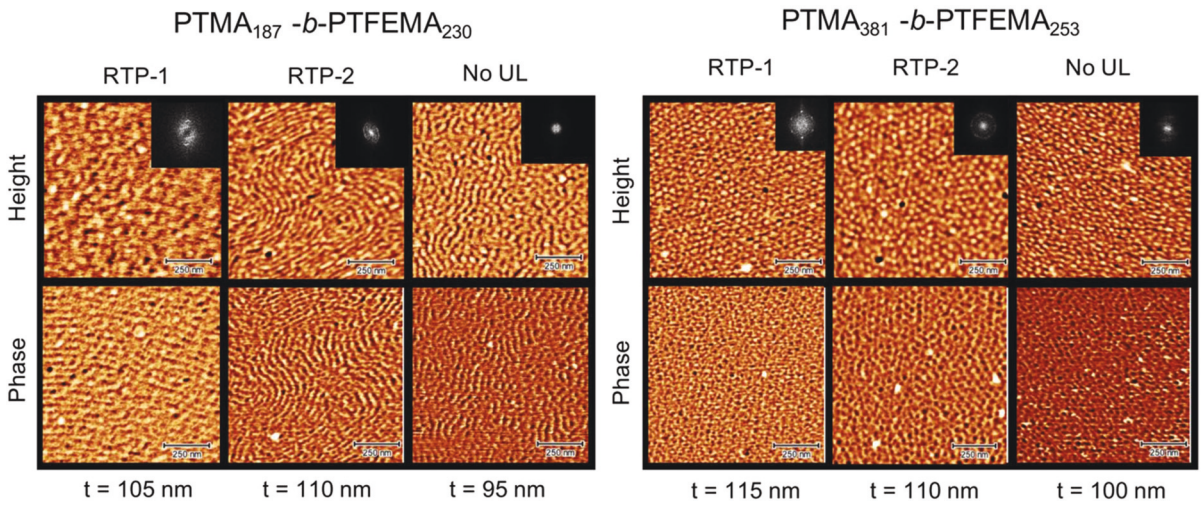

Fig. 3 AFM images of $PTMA_{187}$-*b*-$PTFEMA_{230}$ and $PTMA_{381}$-*b*-$PTFEMA_{253}$ thin films annealed for 6 h in chloroform vapor. The height and phase images are shown are shown for films in which underlayers (RTP-1 and RTP-2) were used, and those which were not. Film thicknesses (t) are noted at the bottom of each figure.

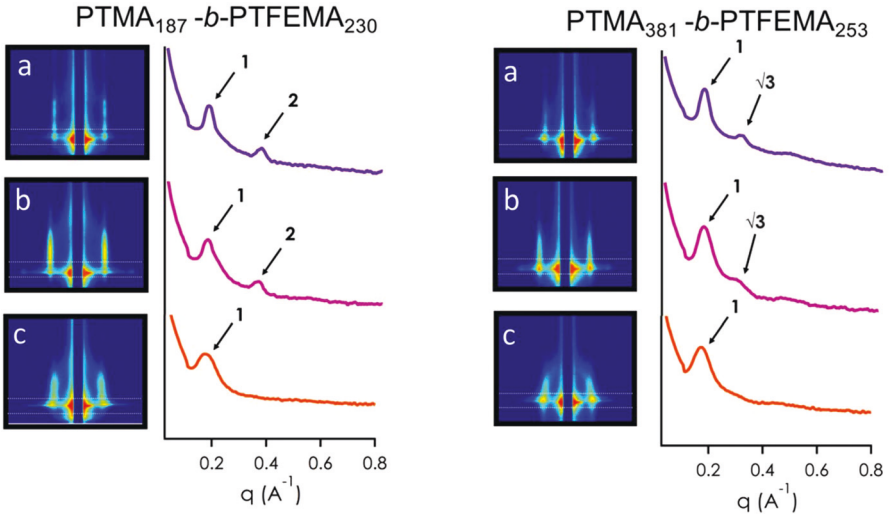

Fig. 4 2D-GISAXS data for $PTMA_{187}$-*b*-$PTFEMA_{230}$ and $PTMA_{381}$-*b*-$PTFEMA_{253}$ thin films annealed for 6 h in chloroform vapor. Data represented showed thin films where (a) RTP-1 was used as an underlayer, (b) RTP-2 was used and (c) no underlayer was used.

Overall, the ordering of these structures is greatly improved when either RTP-1 and RTP-2 are used. The improvement in the long-range order of these two polymers with both neutral underlayers, further corroborates our surface energy estimation of PTMA, which until now, has not been reported in the literature. RTP-2 was synthesized using PiBMA because it has a very similar surface energy to our estimation of PTMA, therefore, it allowed us to also see an improvement in the long-range ordering of the block copolymers.

Phase separation in thin film studies by GISAXS

We also utilize *ex situ* GISAXS to further analyze the phase morphologies of the PTMA-*b*-PTFEMA block copolymer films. GISAXS allows us to determine the structure within the bulk of the film, instead of only at the surface, and has been successfully done for many block copolymer systems, including recently reported PTFEMA-containing block copolymers.[36,37]

Both $PTMA_{187}$-*b*-$PTFEMA_{230}$ and $PTMA_{381}$-*b*-$PTFEMA_{253}$ showed the most ordering due to their high molecular weights. The lower molecular weight polymers reported in this manuscript only showed disordered morphologies with and without neutral underlayers. Both $PTMA_{187}$-*b*-$PTFEMA_{230}$ and $PTMA_{381}$-*b*-$PTFEMA_{253}$ show long-range ordering in the bulk of the film when the polymer films were annealed for 6 hours in $CHCl_3$ vapor and RTP-1 or RTP-2 are used as underlayers. Fig. 4 shows the *ex situ* GISAXS images for $PTMA_{187}$-*b*-$PTFEMA_{230}$ (left) and $PTMA_{381}$-*b*-$PTFEMA_{253}$ (right), along with the intensity profiles integrated along q_y. Prominent first and second order peaks at q_y positions, known as Bragg rods, appear for the samples where neutral layers were used (4a and b). This information allows us to determine both the *d*-spacing of the formed structures and corroborate the type of formed morphology. The q_y ratios between the first and second order peaks were 1 : 2 (lamellar) and 1 : $\sqrt{3}$ (cylindrical) for $PTMA_{187}$-*b*-$PTFEMA_{230}$ and $PTMA_{381}$-*b*-$PTFEMA_{253}$, respectively. The intensity profiles also show us that sample $PTMA_{187}$-*b*-$PTFEMA_{230}$ is of lamellar morphology with domain spacing of 32 nm and $PTMA_{381}$-*b*-$PTFEMA_{253}$ is of cylindrical morphology with domain spacing of 36 nm, as determined by processing methods that allowed us to index refraction peaks corresponding to real-space dimensions.[44]

For the $PTMA_{187}$-*b*-$PTFEMA_{230}$ and $PTMA_{381}$-*b*-$PTFEMA_{253}$ films that did not include an underlayer, only first order peaks perpendicular to q_y are observed (Fig. 4c). This indicates that while there is structure formation during the annealing process, they remain in random orientations throughout the polymer film. This is likely due to the fact that PTFEMA has a lower surface energy compared to PTMA and does not preferentially wet the Si surface, therefore making it difficult for the system to create perpendicularly segregated structures with long-range order. Both RTP neutral layers allowed the surface energy of the substrate to match that of the block copolymers, allowing perpendicular structures to form.

Conclusions

We have demonstrated a facile synthetic route to synthesize PTMA and PTFEMA polymers *via* anionic polymerization using a Na^+/DB18C6 complex as a bulky and sterically hindered countercation. This method allows us to successfully synthesize PTMA-*b*-PTFEMA block copolymers by sequential monomer addition with low dispersities and a broad range of molecular weights. By utilizing neutral underlayers as surface modifiers, (both PTMA-*ran*-PTFEMA-*ran*-PHEMA and PiBMA-*ran*-PTFEMA-*ran*-PHEMA) we have been able to obtain long-range ordering lamellar and cylindrical morphologies, as characterized by AFM and GISAXS. PiBMA was also used as an alternative to PTMA in the neutral layer to provide a more cost-efficient option, as well as to further corroborate the surface

energy estimation of PTMA by the Zisman method, which was found to be 30.1 mJ m^{-2}. The methods reported further expand the synthetic routes to both PTMA and PTFEMA, allowing them to be easily implemented into future materials using anionic polymerization. Our work on stable radical block copolymers shows the potential for controlling the long-range ordering of the stable radical block, suggesting potential applications in nanopatterning of PTMA for future charge transporting solid-state devices.

Conflicts of interest

There are no conflicts to declare.

Acknowledgements

This work was supported by the Department of Energy Office of Basic Energy Science (Grant DE-SC0014336). A. C. would like to acknowledge Ivan Keresztes for his help in acquisition and interpretation of ^{1}H NMR spectra. A. C. is also grateful for a National Science Foundation Graduate Research Fellowship (DGE-1650441). This work made use of the Cornell Center for Materials Research Shared Facilities which are supported through the NSF MRSEC program (DMR-1719875). We acknowledge the use of the Cornell University NMR Facility, which is supported, in part, by the NSF through MRI award CHE-1531632. This work is based upon research conducted at the Cornell High Energy Synchrotron Source (CHESS) which is supported by the National Science Foundation (NSF) under award DMR-1332208. T. H. would like to thank the Grant-in-Aid for Scientific Research (B) (JSPS KAKENHI Grant Number 17H03113), and the Ogasawara Foundation for the Promotion of Science & Engineering. Electron Spin Resonance experiments were completed at ACERT which is supported by the National Institute of General Medical Sciences of the National Institutes of Health (P41GM103521).

Notes and references

1 J. K. Kim, G. Cheruvally, J. H. Ahn, Y. G. Seo, D. S. Choi, S. H. Lee and C. E. Song, *J. Ind. Eng. Chem.*, 2008, **14**, 371–376.
2 G. Hauffman, J. Rolland, J. P. Bourgeois, A. Vlad and J. F. Gohy, *J. Polym. Sci., Part A: Polym. Chem.*, 2013, **51**, 101–108.
3 H. Nishide, S. Iwasa, Y.-J. Pu, T. Suga, K. Nakahara and M. Satoh, *Electrochim. Acta*, 2004, **50**, 827–831.
4 K. Nakahara, S. Iwasa, M. Satoh, Y. Morioka, J. Iriyama, M. Suguro and E. Hasegawa, *Chem. Phys. Lett.*, 2002, **359**, 351–354.
5 K. Nakahara, K. Oyaizu and H. Nishide, *Chem. Lett.*, 2011, **40**, 222–227.
6 Y. Yonekuta, K. Susuki, K. Oyaizu and K. Honda, *J. Am. Chem. Soc.*, 2007, **129**, 14128–14129.
7 L. Rostro, L. Galicia and B. W. Boudouris, *J. Polym. Sci., Part B: Polym. Phys.*, 2015, **53**, 311–316.
8 Y. Zhang, A. Park, A. Cintora, S. R. McMillan, N. J. Harmon, A. Moehle, M. E. Flatté, G. D. Fuchs and C. K. Ober, *J. Mater. Chem. C*, 2018, **6**, 111–118.
9 Y. Joo, V. Agarkar, S. H. Sung, B. M. Savoie and B. W. Boudouris, *Science*, 2018, **359**, 1391–1395.
10 L. Rostro, A. G. Baradwaj, A. R. Muller, J. S. Laster and B. W. Boudouris, *MRS Commun.*, 2015, **5**, 257–263.
11 G. Hauffman, A. Vlad, T. Janoschka, U. S. Schubert and J.-F. Gohy, *J. Mater. Chem. A*, 2015, **3**, 19575–19581.
12 C. Liedel and C. K. Ober, *Macromolecules*, 2016, **49**, 5884–5892.
13 T. Janoschka, A. Teichler, A. Krieg, M. D. Hager and U. S. Schubert, *J. Polym. Sci., Part A: Polym. Chem.*, 2012, **50**, 1394–1407.
14 D. T. Gentekos and B. P. Fors, *ACS Macro Lett.*, 2018, **7**, 677–682.
15 J. M. Widin, A. K. Schmitt, A. L. Schmitt, K. Im and M. K. Mahanthappa, *J. Am. Chem. Soc.*, 2012, **134**, 3834–3844.
16 D. Bendejacq, V. Ponsinet, M. Joanicot, Y.-L. Loo and R. A. Register, *Macromolecules*, 2002, **35**, 6645–6649.
17 N. A. Lynd and M. A. Hillmyer, *Macromolecules*, 2005, **38**, 8803–8810.
18 N. A. Lynd and M. A. Hillmyer, *Macromolecules*, 2007, **40**, 8050–8055.
19 J. M. Widin, M. Kim, A. K. Schmitt, E. Han, P. Gopalan and M. K. Mahanthappa, *Macromolecules*, 2013, **46**, 4472–4480.
20 M. W. Matsen, *Phys. Rev. Lett.*, 2007, **99**, 1–4.
21 T. Katsumata, M. Satoh, J. Wada, M. Shiotsuki, F. Sanda and T. Masuda, *Macromol. Rapid Commun.*, 2006, **27**, 1206–1211.
22 J. Qu, T. Katsumata, M. Satoh, J. Wada and T. Masuda, *Polymer*, 2009, **50**, 391–396.
23 T. Sukegawa, A. Kai, K. Oyaizu and H. Nishide, *Macromolecules*, 2013, **46**, 1361–1367.
24 K. Oyaizu, T. Sukegawa and H. Nishide, *Chem. Lett.*, 2011, **40**, 184–185.
25 P. Nesvadba, L. Bugnon, P. Maire and P. Novák, *Chem. Mater.*, 2010, **22**, 783–788.
26 K. Koshika, N. Sano, K. Oyaizu and H. Nishide, *Macromol. Chem. Phys.*, 2009, **210**, 1989–1995.
27 M. Suguro, S. Iwasa and K. Nakahara, *Macromol. Rapid Commun.*, 2008, **29**, 1635–1639.
28 K. Murakami and J. Sohma, *J. Phys. Chem.*, 1978, **82**, 2825–2828.
29 O. H. Griffith, J. F. W. Keana, S. Rottschaefer and T. A. Warlick, *J. Am. Chem. Soc.*, 1967, **89**, 5072.
30 J. Allgaier and H. Finkelmann, *Macromol. Rapid Commun.*, 1993, **14**, 267–271.
31 T. Sukegawa, H. Omata, I. Masuko, K. Oyaizu and H. Nishide, *ACS Macro Lett.*, 2014, **3**, 240–243.
32 M. A. Hillmyer and T. P. Lodge, *J. Polym. Sci., Part A: Polym. Chem.*, 2002, **40**, 1–8.

33 I. J. Park, S.-B. Lee and C. K. Choi, *J. Appl. Polym. Sci.*, 1994, **54**, 1449–1454.
34 D. R. Iyengar, S. M. Perutz, C.-A. Dai, C. K. Ober and E. J. Kramer, *Macromolecules*, 1996, **29**, 1229–1234.
35 N. M. L. Hansen, K. Jankova and S. Hvilsted, *Eur. Polym. J.*, 2007, **43**, 255–293.
36 R. Nakatani, H. Takano, A. Chandra, Y. Yoshimura, L. Wang, Y. Suzuki, Y. Tanaka, R. Maeda, N. Kihara, S. Minegishi, K. Miyagi, Y. Kasahara, H. Sato, Y. Seino, T. Azuma, H. Yokoyama, C. K. Ober and T. Hayakawa, *ACS Appl. Mater. Interfaces*, 2017, **9**, 31266–31278.
37 A. Chandra, R. Nakatani, T. Uchiyama, Y. Seino, H. Sato, Y. Kasahara, T. Azuma and T. Hayakawa, *Adv. Mater. Interfaces*, 2019, **1801401**, 1–7.
38 R. Maeda, T. Hayakawa and C. K. Ober, *Chem. Mater.*, 2012, **24**, 1454–1461.
39 C. Liedel, A. Moehle, G. D. Fuchs and C. K. Ober, *MRS Commun.*, 2015, **5**, 441–446.
40 T. Narita, *Prog. Polym. Sci.*, 1999, **24**, 1095–1148.
41 T. Narita, T. Hagiwara, H. Hamana, H. Yanagisawa and Y. Akazawa, *Makromol. Chem.*, 1986, **187**, 739–744.
42 T. Narita, T. Hagiwara, H. Hamana, T. Miyasaka, A. Wakayama and T. Hotta, *Makromol. Chem.*, 1987, **188**, 273–279.
43 A. Nagaki, K. Akahori, Y. Takahashi and J. Yoshida, *J. Flow Chem.*, 2014, **4**, 168–172.
44 D.-M. Smilgies and D. R. Blasini, *J. Appl. Crystallogr.*, 2007, **40**, 716–718.
45 I. In, Y. H. La, S. M. Park, P. F. Nealey and P. Gopalan, *Langmuir*, 2006, **22**, 7855–7860.
46 D. Baskaran, *Prog. Polym. Sci.*, 2003, **28**, 521–581.
47 W. E. Goode, F. H. Owens and W. L. Myers, *J. Polym. Sci.*, 1960, **47**, 75–89.
48 D. L. Glusker, I. Lysloff and E. Stiles, *J. Polym. Sci.*, 1961, **49**, 315–334.
49 F. J. Gerner, H. Höcker, A. H. E. Müller and G. V. Schulz, *Eur. Polym. J.*, 1984, **20**, 349–355.
50 S. Maleknia and J. Brodbelt, *J. Am. Chem. Soc.*, 1992, **114**, 4295–4298.
51 S. K. Varshney, R. Jerome, P. Bayard, C. Jacobs, R. Fayt and P. Teyssie, *Macromolecules*, 1992, **25**, 4457–4463.
52 P. D. J. Grootenhuis, J. Van Eerden, E. J. R. Sudholter, D. N. Reinhoudt, A. Roos, S. Harkema and D. Feil, *J. Am. Chem. Soc.*, 1987, **109**, 4792–4797.
53 S. Wu, *J. Polym. Sci., Part C: Polym. Symp.*, 2007, **34**, 19–30.
54 T. Xu, C. J. Hawker and T. P. Russell, *Macromolecules*, 2005, **38**, 2802–2805.
55 V. Khanna, E. W. Cochran, A. Hexemer, G. E. Stein, G. H. Fredrickson, E. J. Kramer, X. Li, J. Wang and S. F. Hahn, *Macromolecules*, 2006, **39**, 9346–9356.
56 E. Han, K. O. Stuen, Y. H. La, P. F. Nealey and P. Gopalan, *Macromolecules*, 2008, **41**, 9090–9097.

